

SANS STUDIES OF INTERACTING HEMOGLOBIN IN INTACT ERYTHROCYTES

S. KRUEGER* AND R. NOSSAL†

**Department of Physics and Astronomy, University of Maryland, College Park, Maryland 20742, and National Bureau of Standards, Gaithersburg, Maryland 20899, and †Physical Sciences Laboratory, Division of Computer Research and Technology, National Institutes of Health, Bethesda, Maryland 20892*

ABSTRACT Small angle neutron scattering (SANS) was used to investigate interaction forces between hemoglobin (Hb) molecules contained within human red cells. The scattering separately attributable to cell membranes and intracellular Hb was identified. A series of D₂O-H₂O contrast variation measurements were made in order to establish conditions for which scattering from the cell membrane is minimized (~15% D₂O). Measurements then were performed to examine changes in intermolecular Hb interactions occurring when the cells are contracted or swollen by varying the ionic strength of the suspension buffer. The scattering cross-sections were fitted to structure factors computed by a mean spherical approximation, and molecular parameters thereby extracted. Oxygenation studies on normal cells were performed, and results contrasted with those of similar studies of erythrocytes obtained from sickle cell disease patients.

INTRODUCTION

Small-angle neutron scattering (SANS) can be used to study intermolecular interactions occurring within highly concentrated protein solutions (1). The volume fraction occupied by the scatterers, their effective size, and various parameters related to electrostatic interactions can be determined by fitting scattering cross-sections to calculated interparticle structure factors. The applicability of this technique for studying core proteins in intact biological vesicles, as epitomized by investigations of hemoglobin contained in human erythrocytes, now will be illustrated.

When biological vesicles are examined by SANS, considerable scattering from membranous hydrocarbon structures can occur which might obscure that from protein cores. However, most of this scattering can be eliminated by the method of contrast variation, which has been used successfully in SANS studies of macromolecular structure of two-component systems. A simple adjustment of D₂O-H₂O ratio in the solvent allows each component to be separately probed without perturbing the particle as a whole. That H₂O and D₂O have very different scattering densities makes it possible to adjust the solvent conditions to match those of one component, which leaves only the other component visible to the neutrons. It is this method that permitted the determination of nucleic acid structure relative to protein structure in nucleosomes (2) and ribosomes (3).

Intact red blood cells (RBCs) are not two-component systems in the strictest sense. The membrane itself is not a single component but consists of both lipid and protein. Solvent conditions cannot be found that completely elimi-

nate membrane scattering, as the lipid-protein boundaries are not well defined. However, the intensity of the scattering due to the membrane can be minimized, allowing that due to the protein core to be more easily measured.

In certain instances, the range of angles where membrane scattering is significant may be quite different from that where protein scattering is important. However, when larger protein complexes are present, membrane scattering may hide that which arises from the protein. In this instance it is important to diminish the membrane scattering as much as possible. Thus, the motivation for developing a contrast variation technique for studying biological vesicles is clear. If the membrane scattering can be minimized, the core contents can be studied in situ. It might then be possible to study various aspects of vesicle physiology. In the case of human erythrocytes, for example, consequences of changing various transmembrane transport parameters could be investigated.

The procedures devised for this purpose are discussed extensively in the following section (Methods). The scattering cross-sections for the core molecules are fit to curves calculated by a mean spherical approximation (MSA) for the structure factor pertaining to interacting charged hard-sphere particles. Computer codes that first were developed for analyzing the scattering from micelle suspensions (4, 5) and subsequently applied to studies of concentrated protein solutions (1, 6) were employed. Changes that need to be effected because the protein core particles are segregated within vesicles, rather than being uniformly distributed throughout the scattering volume are discussed. Also described is a fitting procedure for

determining the protein and membrane D₂O-H₂O contrast match points.

The status of the intracellular Hb was investigated by adjusting the D₂O content of the solution to that of the membrane matchpoint. To illustrate the methodology, data are provided that show how variations in cell volume and oxygen tension can affect hemoglobin electrostatic charge and intermolecular associations (see Results and Discussion). These results are of interest when interpreting data obtained from light scattering experiments performed on single cells (7, 8). Finally, cross-section data that indicate the possibility of observing polymerization of Hb S in erythrocytes obtained from sickle cell disease patients are presented.

Sample Preparation

Human erythrocytes from healthy donors were obtained by extraction from citrated whole blood (~0.5% Na Citrate, wt/vol). Peripheral blood was diluted 1:1 with phosphate-NaCl buffer (150 mM NaCl, 5 mM NaH₂PO₄, 0.02% Na EDTA, titrated to pH 7.33 with NaOH) and spun at 1,600 rpm for 10 min in an IEC model HN-S (Damon Corp., Needham Heights, MA) centrifuge (step 1). The supernatant containing the diluted plasma, as well as the "buffy coat" at the top of the packed red cells, was discarded. This procedure was repeated twice (step 2). In initial studies the packed cells were resuspended 1:3 in a similar phosphate-NaCl buffer made up in D₂O (titrated to a pH meter reading of 6.93, the difference of 0.4 pH units arising from differing electrode sensitivity [9]), and left on ice for 3 h (step 3). This procedure was repeated several times (step 4) over a 24 h period in order to ensure that almost all exchangeable hydrogen ions were diluted and washed out of the sample. (The original H⁺ content of the buffer was diluted at least 150 times by the combination of the wash procedures.) Finally, the cells were resuspended to a final concentration at ~1.3 times the initial whole blood hematocrit (step 5).

When cells were prepared for contrast variation measurements, the sample was separated into two equal aliquots after step 2. After the D₂O sample was prepared, the remaining portion was centrifuged and the cells resuspended into a volume of H₂O buffer equal to that of the D₂O sample; this assured that when the two suspensions were mixed, in order to make samples containing differing amounts of D₂O, the RBC concentration would be invariant.

In later studies requiring "fresh" cells suspended in a buffer containing 15% D₂O (i.e., conditions near the membrane match point), steps 3 and 4 were omitted from the sample preparation but all washes were performed in a buffer made up to the desired final concentration of D₂O. The buffer acidity was determined by assuming the pH equivalent of a 15% D₂O buffer can be calculated as $\text{pH}_{\text{equiv}} = 0.85 \text{ pH}_m + 0.15 (\text{pH}_m + 0.4) = \text{pH}_m + 0.06$, where pH_m is that value indicated by a conventional pH

meter. Because the preparation time accordingly was shortened, a small amount of H⁺-D⁺ exchange continued to occur after initial measurements were made; this slightly affected the background corrections to the cross section, but was easily accommodated by our data fitting routines (see Results and Discussion).

Similar procedures were used to obtain cell suspensions in buffers of differing osmolarity. Samples used for oxygenation-deoxygenation studies also were prepared as indicated above except that, after removing an aliquot for the "oxy" cell measurements, water saturated nitrogen was bubbled through the cell suspension. After 20 min the cells, which were contained in a Vacutainer tube (Becton Dickinson, Rutherford, NJ), had acquired a deep purple coloration. The cell suspension then was transferred with a gas-tight syringe, through a septum, into a cuvette that had been extensively flushed with nitrogen. No attempt was made to obtain a precise measure of the oxygen tension in this, the "deoxy," sample. In some instances cells were reoxygenated by placing them in an open test-tube and swirling them on the side of the tube for ~10 min.

A suspension of RBC membrane ghosts and membrane fragments in 100% D₂O buffer was prepared by a modification of a procedure originally devised by Dodge (10). After washing the cells several times in D₂O buffer according to the procedures discussed above, the cells were lysed by suspending them in 20 Mosm D₂O buffer (i.e., normal D₂O buffer diluted 1:30 in D₂O). The sample then was spun in a J21 centrifuge, JA20 rotor (Beckman Instruments, Inc., Palo Alto, CA), for 10 min at 12,000 rpm, followed by a 35 min spin at 17,000 rpm. The supernatant was gently removed by pouring, the pellet was resuspended in 20 mOsm D₂O buffer, and the specimen again centrifuged for 40 min at 17,000 rpm. Finally, the supernatant was carefully aspirated with a Pasteur pipette and the pellet resuspended in normal D₂O buffer. The pellet was a pale pink, indicating possibly that trace amounts of Hb remained bound to the membranes. A few small clumps of membranes and ghosts, perhaps induced by the D₂O, were visible in the suspension; for our purposes, however, it was not necessary to obtain intact, closed, RBC ghosts.

An erythrocyte sample obtained from a sickle cell disease patient was prepared by a similar procedure, except that the cells were extracted in normal H₂O buffer. D₂O then was added, to a final concentration of 10%, which slightly diluted the buffer. The washed sickle RBCs were obtained from the National Institutes of Health Blood Bank with the kind assistance of Dr. R. Davies.

Neutron Measurements

Scattering was performed on the SANS spectrometer at the National Bureau of Standards (11). The average wavelength used was $\lambda = 6.0 \text{ \AA}$ with a spread of $\Delta\lambda/\lambda = 25\%$. Neutrons were collimated using the standard coarse collimation, i.e., an entrance circular pinhole of $d_1 = 2.70 \text{ cm}$, a second pinhole of $d_2 = 1.80 \text{ cm}$ at a distance of 410 cm from

the first, and a third pinhole of $d_3 = 1.27$ cm at the sample chamber position. Samples were measured in quartz cells having a volume of ~ 0.30 ml and path length of 1.0 mm. A 64×64 cm² position-sensitive detector with 128×128 pixels (12), each defining a scattering angle Θ_{ij} , was used to intercept the scattered neutrons. A sample-to-detector distance of 3.60 m was used. The detector center was placed at a 3.5° angle in order that a range of Bragg wave number, $Q = 4\pi\lambda^{-1} \sin(\Theta/2) = 0.0128\text{--}0.1650 \text{ \AA}^{-1}$, could be covered. Data were corrected for empty cell and background as well as incoherent scattering of the solvent by the method of Chen and Bendedouch (13). Scattering intensities were put on an absolute scale by calibrating against the scattering from a standard silica-gel sample, for which the absolute cross-section had been previously calculated. Corrected and rescaled data from each pixel were then radially averaged. This averaged cross-section per unit volume is denoted $I(Q) = d\Sigma(Q)/d\Omega$.

Experimental Procedures and Methods of Data Analysis

The positions of the protein molecules in a dense solution are not independent of one another, becoming less so as the distance between particles decreases. This gives rise to an interference effect that changes the shape of the scattering profile. Small deviations from dilute scattering cross-sections can often be detected when concentrations reach about 10 mg/ml, with larger deviations becoming more noticeable as the concentration continues to increase. The average intracellular concentration of Hb in RBCs is ~ 330 mg/ml, so interference scattering must be taken into account in the data analysis.

To a first approximation, the differential cross-section per unit volume for protein scattering may be written (6)

$$I(Q) = KN_p(\Delta\rho)^2 V_p^2 P(Q) S'(Q), \quad (1)$$

where N_p is the number of protein molecules per unit volume in the solution, V_p is the volume occupied by a single protein molecule and $\Delta\rho = |\bar{\rho}_p - \rho_s|$, the "contrast," is the difference between the average scattering density of the protein and that of the solvent. K is the fraction of the solution actually occupied by the protein cores of the cells. $P(Q)$ is the "particle structure factor" representing the scattering from a single core particle averaged over all orientations and normalized such that $P(0) = 1$. $S'(Q)$ is the "averaged interparticle structure factor" which accounts for the interference scattering between particles. For a dilute solution, $S'(Q) = 1$ for all Q . It is important to note that $I(Q)$, as defined above, refers to the scattering from a monodisperse solution of proteins located in the cores of a suspension of biological vesicles or cells.

Since hemoglobin is a spherical molecule, $P(Q)$ is easily calculated. $S'(Q)$ can be computed by solving the Ornstein-Zernicke equation (14) in a mean spherical approxi-

mation (15) when the interparticle potential consists of a hard core and a Yukawa potential tail. An analytic solution for this case, which is based on the DLVO theory of interacting colloidal particles, has been provided by Hayter and Penfold (4, 5) and their FORTRAN subroutine has been incorporated into a program (16) which fits the data to the theoretical $I(Q)$ given by Eq. 1. Further modification of the program by the present authors (17) allows a broad choice of fitting parameters. Possible fitting parameters are η , A_k , Gek, Amp, R , and Bck, defined as follows.

R is the particle radius and Bck is the background due to incoherent scattering. This background is usually small since the incoherent scattering from the H₂O in the solvent is subtracted from the total scattering obtained from solvent plus sample. Therefore, the background scattering arises only from the hydrogen in the cell components. η is the packing fraction of the protein within the cells, given as

$$\eta = \frac{N_p \pi \sigma^3}{6}, \quad (2)$$

where σ is the equivalent hard sphere diameter of the protein ($\sigma = 2R$). A_k is the dimensionless parameter $\kappa\sigma$, where κ , the Debye screening constant, is related to the ionic strength, I , of the solution as

$$\kappa = \left(\frac{8\pi e^2 I N_A}{10^3 \epsilon k_B T} \right)^{1/2}, \quad (3)$$

where N_A is Avogadro's number, ϵ is the dielectric constant of the solution, k_B is the Boltzmann constant, and T is the absolute temperature. The quantity Gek is given as (c.f., Eq. 1)

$$\text{Gek} = \frac{Z^2 e^2}{\epsilon k_B T \sigma (1 + A_k/2)^2}, \quad (4)$$

where Ze is the charge on the particle. The amplitude, Amp, is given as

$$\text{Amp} = KN_p(\Delta\rho)^2 V_p^2. \quad (5)$$

Notice that K depends on the packing fraction of the cells and on the fraction of the cell volume occupied by the protein core. For example, if the cells were spherical and packed such that they were touching, the packing fraction would be equal to 0.74 which is the maximum packing fraction for closely packed spheres in a face-centered cubic lattice structure. If, in addition, 100% of the cell volume was occupied by core protein, then $K = 0.74$. For spherical cells, this is the maximum possible value for K . Normally, since cell cores occupy a much smaller portion of the cell volume, K is even smaller. For this reason, even when the cells are not spherical, as in the case of RBCs, K will be < 1 . Consequently, the scattering amplitude for a given concentration of proteins in the cell cores will be less than that of a solution of protein at the same concentration.

The parameters Gek, η and A_k directly affect the shape

of the structure factor, $S'(Q)$, as shown in Fig 1. It follows from Eq. 1 that these parameters determine the shape of $I(Q)$ as well. On the other hand, the parameter R affects the shape of $I(Q)$ without having any effect on $S'(Q)$ at all. The changes each parameter makes to $I(Q)$ are illustrated in Fig. 2.

To apply the above theory to RBCs, it is desirable to minimize the membrane scattering as much as possible so that the protein contrast will be large compared with that of the membrane. In the case of RBCs the procedure is simplified by the fact that the important features of the membrane and protein portions of the scattering curve occur at different values of Q . While the membrane scattering is insignificant beyond $Q \approx 0.06 \text{ \AA}^{-1}$, the protein scattering is maximal at $Q \approx 0.09 \text{ \AA}^{-1}$. Therefore, a series of contrast variation measurements on the intact cells contains sufficient information to determine the membrane match point. The protein match point also can be verified if desired.

First, the data from the contrast variation measurements are fit for values of $Q > 0.06 \text{ \AA}^{-1}$ by using the MSA theory for the protein. Even if the membrane contrast is much greater than that of the protein, the fits should be sufficiently accurate for determining the match point. After determining the best fit from the data at large Q values, the entire curve $I_p(Q)$ is calculated according to the MSA theory. The complete calculated curve $I_p(Q)$ then is subtracted from the experimentally determined $I(Q)$ in order to obtain $I_m(Q)$, which pertains to membrane scattering. $I_m(Q)$ is fit by using a flat sheet approximation (18) whereby the membrane is represented by a flat sheet with constant thickness, t , and two other, much larger, dimensions. The scattering intensity $I_m(Q)$ can be separated into a factor proportional to Q^{-2} and a second "thickness factor" such that

$$I_m(Q) = \frac{I_0}{Q^2} e^{-Q^2 R_t^2}, \quad (6)$$

where R_t is just equivalent to $t/\sqrt{12}$ and I_0 is a constant to be fit to the data. Both sides of Eq. 6 are multiplied by Q^2

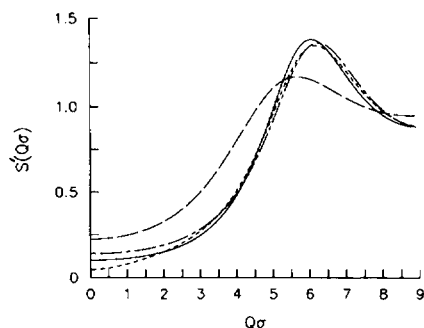


FIGURE 1 Model calculations illustrating the effect of varying the parameters η , G_{ek} and A_k on $S'(Q\sigma)$. (—) $\eta = 0.25$, $G_{ek} = 1.0$, $A_k = 6.0$ (base values); (---) $\eta = 0.15$, $G_{ek} = 1.0$, $A_k = 6.0$; (-·-) $\eta = 0.25$, $G_{ek} = 0.01$, $A_k = 6.0$; (···) $\eta = 0.25$, $G_{ek} = 1.0$, $A_k = 1.0$.

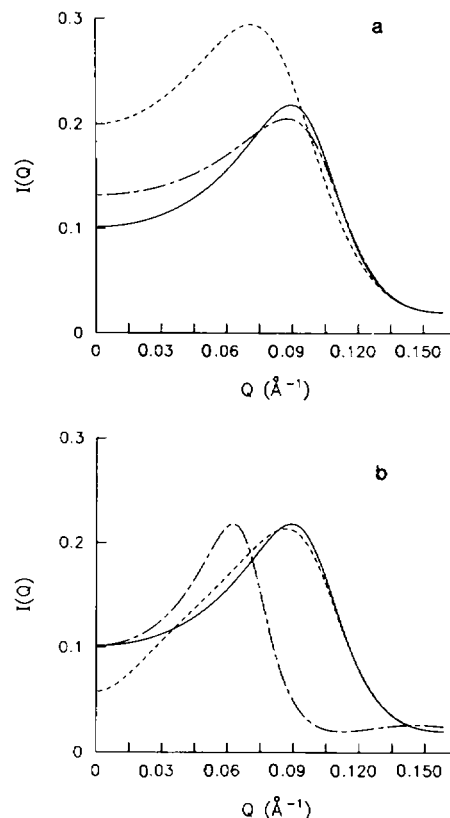


FIGURE 2 Model calculations illustrating the effect of varying the parameters η , G_{ek} , A_k and R on $I(Q)$. (a, b) (—) $\eta = 0.25$, $G_{ek} = 1.0$, $A_k = 6.0$, $R = 28.0 \text{ \AA}$ (base values). (a) (---) $\eta = 0.15$, $G_{ek} = 1.0$, $A_k = 6.0$, $R = 28.0 \text{ \AA}$; (-·-) $\eta = 0.25$, $G_{ek} = 0.01$, $A_k = 6.0$, $R = 28.0 \text{ \AA}$; (···) $\eta = 0.25$, $G_{ek} = 1.0$, $A_k = 1.0$, $R = 28.0 \text{ \AA}$; (---) $\eta = 0.25$, $G_{ek} = 1.0$, $A_k = 6.0$, $R = 40.0 \text{ \AA}$.

and the natural log is taken. A plot of $\ln [I_m(Q) \cdot Q^2]$ vs. Q^2 results in a straight line with slope $-R_t^2$ and intercept $\ln(I_0)$. From these values, t and I_0 are obtained. A plot of $(I_0)^{1/2}$ vs. %D₂O should yield a straight line crossing the x-axis at the membrane match point. Similarly, a plot of $(\text{Amp})^{1/2}$ (see Eq. 5) vs. %D₂O should provide a straight line crossing the x-axis at the protein match point.

In the case of RBCs, it is desirable to take data at the membrane "match point," as the protein contrast is maximum there when compared with that of the membrane. The protein scattering cross-section, $I_p(Q)$, can be determined by using the MSA fitting procedure. Changes occurring, for example, upon deoxygenation or variation of solvent ionic strength can be documented by observing changes in the various fitting parameters.

RESULTS AND DISCUSSION

In Fig. 3, the scattering profile from a normal RBC sample is compared with that from a preparation of RBC membrane fragments. These samples were washed and suspended in 100% D₂O, conditions where incoherent scattering from hydrogen atoms in the solvent should be

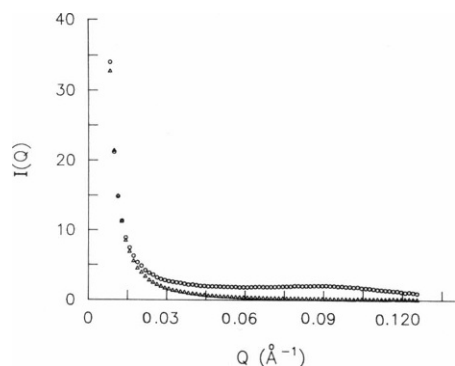


FIGURE 3 Comparison between scattering from intact RBCs and membranes (100% D₂O), showing that the scattering from the Hb within the cells can be distinguished. (O) Cells; (Δ) membranes.

minimized. The data indicate that membrane scattering is negligible for $Q \geq 0.06 \text{ Å}^{-1}$.

Scattering cross-sections obtained during contrast variation measurements on RBCs are shown in Fig. 4. These data suggest that the membrane match point is between 10–20% D₂O. The protein portion of the RBC scattering profile, having a peak near $Q = 0.09 \text{ Å}^{-1}$, indeed becomes more pronounced in comparison with the membrane portion when the cells are suspended in H₂O as well as in buffer that contains 10 and 20% D₂O. Note that the protein peak is unobservable in the 30 and 40% D₂O samples. Although the intensity of the protein scattering discerned in the 70 and 100% D₂O samples is large

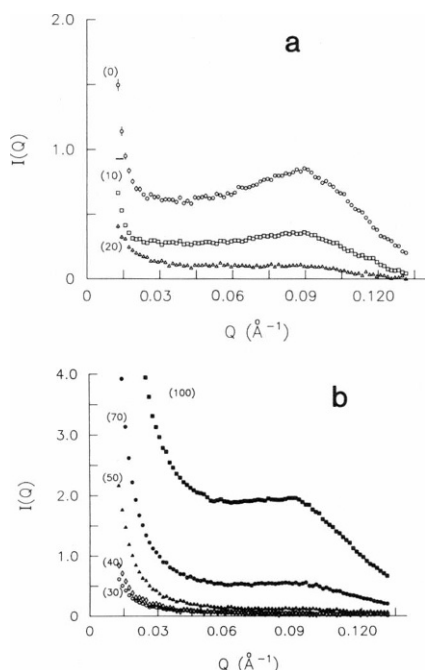


FIGURE 4 Contrast variation data, taken to establish optimal conditions for observing Hb interactions. (a, b) Scattering cross-sections for differing D₂O percentages (in parentheses), plotted on an absolute scale. Error bars for each data set are similar to those shown for the 0 and 20% D₂O cases.

compared with that of the rest of the contrast variation series, the protein scattering is in those cases much less than the membrane scattering. It is desirable to eliminate the membrane contribution as much as possible. Note that although the intensity of the protein scattering is lowered in 10 or 20% D₂O, the membrane scattering is reduced by an even greater amount.

To calculate the protein and membrane match points, MSA fits were made to the large Q (i.e., $Q \geq 0.06 \text{ Å}^{-1}$) regions of the curves for RBCs in 0, 10, 20, 50, 70, and 100% D₂O. Because protein scattering cross-sections are small compared with membrane scattering in 50, 70, and 100% D₂O, the MSA fits were somewhat uncertain for those conditions. However, the fitted MSA amplitudes, Amp, are relatively insensitive to slight variations in the shape of the scattering cross-sections. A plot of $(\text{Amp})^{1/2}$ vs. %D₂O (see Fig. 5) places the Hb match point at ~39% D₂O, in good agreement with results of earlier studies on Hb (19). It is significant that the MSA fitting procedure can be used to determine contrast match points even when the solute concentrations are very high. (For convenience in representing data in Fig. 5, results have been normalized to a value of -1.0 at 100% D₂O concentration.)

Model calculations of the entire scattering cross-section for the protein, $I_p(Q)$, were made for each solution condition by using the parameters of the best fit to the corresponding "large Q " data. The calculated $I_p(Q)$ then was subtracted from $I(Q)$ in each case, yielding the scattering cross-sections $I_m(Q)$ for the membranes alone. A plot of normalized values of $(I_0)^{1/2}$ vs. %D₂O, (see Fig. 5) shows that the membrane "match point" lies between 14

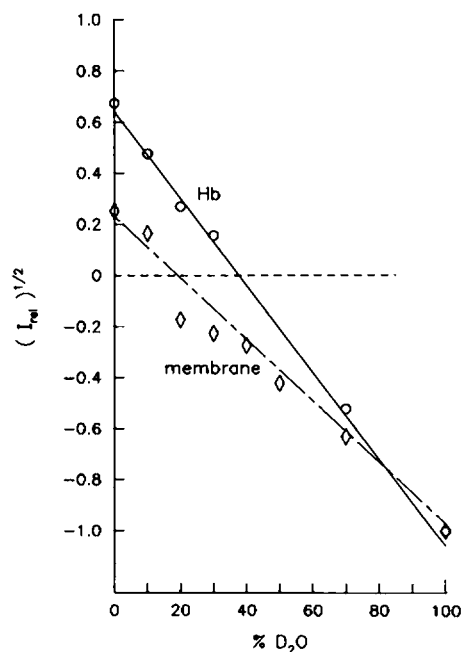


FIGURE 5 Amplitudes of separate scattering components (normalized to -1.0 at 100% D₂O concentration), illustrating the approximate membrane and protein match points.

and 18% D₂O (c.f., Eq. 6). All further experiments were performed with RBCs in 15% D₂O where the contribution of the membrane to the total scattering is minimized.

Fig. 6 illustrates the scattering profiles for RBCs in normal buffer (300 mOsm), as well as in "low salt" buffer (150 mOsm), and "high salt" buffer (600 mOsm). When the ionic strength of the solution is increased from that of the normal buffer, the cells shrink. Conversely, a decrease in ionic strength causes the cells to swell. In both cases, the concentration of Hb inside the cells changes, producing a corresponding change in η because the latter depends on N_p (c.f., Eq. 2). When the cells swell, the volume fraction η decreases, but it increases as the cells shrink. This is clearly evident in the results shown in Table I, where values of the parameters that correspond to the best fits of the data are presented. The closer packing of the Hb molecules in the latter case also causes a decrease in the isothermal compressibility of the solution, resulting (20) in a lower value of $S'(0)$. Fig. 7 illustrates this decrease in $S'(0)$ as the ionic strength of the solution is increased.

The present studies indicate that a small decrease in the effective radius, R , of the core protein occurs upon increasing the ionic strength of the solution and, hence, the concentration of intracellular Hb (see Table I). As the Hb molecules are forced to pack closer together, the interaction diameter should approach the actual diameter of a "bare" Hb molecule. A large increase in charge, Z , also is noted as the ionic strength increases. To calculate Z from the data we assume that the cellular ionic strength, I , is approximately equal to that in the buffer, i.e., that the cells act as perfect osmometers. From a physical point of view, an increase in Z is expected, since additional salt in the solution causes greater screening of the charge on each Hb molecule, making it more likely that the Hb molecule can hold that charge. The concentration of cations that can bind to the Hb molecules presumably also increases. On the other hand, if no other factors were to change, an increase in intracellular Hb concentration would cause an

TABLE I
RED BLOOD CELLS UNDER VARYING SALT
CONDITIONS 15% D₂O BUFFER pH 7.4

	η	A_k	Gek	Z	Amp	R	Bck
High salt (600 mOsm)	0.286	10.2	1.4	20	0.40	26.8	0.017
Normal salt (300 mOsm)	0.223	7.2	0.9	12	0.88	27.8	0.020
Low salt (150 mOsm)	0.166	5.1	0.2	4	0.92	28.4	0.004

N_p , the number of cells per unit volume, remained constant as the salt conditions were varied. The statistical errors associated with the fitting procedure are as follows: $\eta(\pm 0.002)$; Gek(± 0.1); Z(± 1); Amp(± 0.01); R(± 0.1); Bck(± 0.001).

increase in the total electrostatic interaction energy as the distance between molecules decreases. This would tend to decrease the net charge on the Hb molecules (21).

Quasielastic light scattering studies of single erythrocytes performed under similar conditions (7) suggest that, when the cells are swollen, intracellular hemoglobin exists predominantly as monomers. Hemoglobin aggregates, if present, are small and relatively few. As the cells shrink, an increasing percentage of the Hb seemingly becomes incorporated into large aggregates (7). Those studies also suggest that the cell-to-cell variability of the state of the Hb molecules increases as the cells shrink. Assuming that the average Hb concentration within cells under normal salt conditions is 330 mg/ml, the volume fraction η can be calculated by Eq. 2 to be 0.272, using $R = 28 \text{ \AA}$ and $M = 67,000$, i.e., all Hb molecules exist as monomers. This exceeds the fitted value by $\sim 18\%$, which according to Eq. 2 corresponds to a concentration of 276 mg/ml. This discrepancy is consistent with that found for concentrated Hb solutions (unpublished results). In that case, the higher the Hb concentration, the larger is the discrepancy between the fitted η and the calculated value corresponding to that concentration; at concentrations near 300 mg/ml, how-

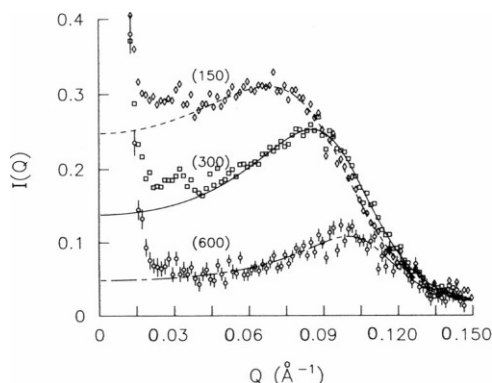


FIGURE 6 RBCs in 15% D₂O buffer (pH 7.4) of differing osmolarity (mOsm, in parentheses). The lines represent calculated Hb scattering cross-sections based on the parameters of best fit to the data for $Q \geq 0.06 \text{ \AA}^{-1}$. The background values were normalized to 0.02. Similar error bars are found for each data set.

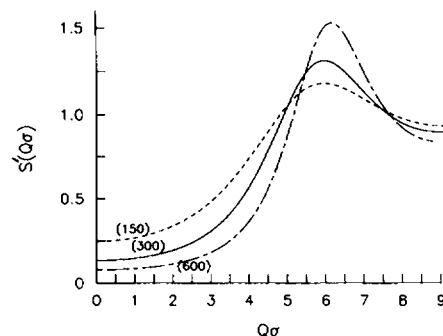


FIGURE 7 Calculated $S'(Q\sigma)$ for Hb, based on the parameters of best fit for $Q \geq 0.06 \text{ \AA}^{-1}$. Note the large changes in Hb interactions that occur when cell volumes change in response to modification of the external buffer. (Osmolarity values in parentheses.)

ever, the discrepancy in the Hb solutions is much greater than that noted here in the RBCs in normal buffer.

A lowered apparent volume fraction would result from the MSA data fitting scheme if some Hb molecules dimerized or formed higher-order associations. The scattering from such larger entities would increase the relative amplitude of the cross-section at lower values of Q . Thus, when the MSA fitting program is employed, the parameter η , which is determined largely by the shape of $I(Q)$ closer to $Q = 0$, would appear to be smaller than the actual value. On the other hand, the parameter R , which is determined largely by fitting to the shape of $I(Q)$ at large Q values, is not sensitive to such associations. If present, the form factors for dimers and higher oligomers decay towards zero at much smaller values of Q . The data shown in Table I suggest that the discrepancy between fitted and calculated values, arising from additional molecular associations, increases when the RBC volume decreases (assuming that the ratio of cell volumes is approximately inversely proportional to the solution osmolarity). This influence is in accord with the earlier light scattering results obtained from single RBCs (8). It should be noted that similar discrepancies do not seem to arise in SANS studies of dense solutions of BSA (1) or cytochrome *c* (22).

One possible complication involves the decrease in scattering amplitude that is evident when the salt concentration of the solution is increased (see Fig. 6). Although N_p changes as the cell volume varies, KN_p should remain constant if the number of cells per unit volume remains constant. For these measurements, the number of cells per unit volume was adjusted to be approximately the same for each of the three buffers. Therefore, Eq. 5 indicates that there should be no change in amplitude. Yet, a marked decrease in amplitude is evident as the concentration of Hb within the cells increase, consistent with earlier studies of highly concentrated BSA solutions (1) and more recent

studies of Hb solutions (unpublished results). It is possible that some settling of the cells occurred during measurement, especially in the "high salt" case. However, a more likely explanation is that Eqs. 1 and 5 are approximations and that additional factors need to be taken into account.

The changes in the scattering profile that occur upon deoxygenation of the Hb within the RBCs are illustrated in Fig. 8. The corresponding parameters of best fit are listed in Table II. These values were computed by making fits in three Q -ranges, each with a maximum Q value of 0.1645 and minimum Q value of 0.0459, 0.0609, and 0.0759, and then averaging the results. The expected errors represent the standard deviation about the average values. Data were taken on freshly prepared cells, within 4 h after the blood was drawn. These cells were measured again the next day. Finally, both the oxygenated and deoxygenated samples were reoxygenated in order to verify that the deoxy cells were not physically changed during the deoxygenation process. The fits for both the oxy and deoxy cells become essentially identical upon reoxygenation and thus, it can be assumed that changes seen in the Hb parameters upon deoxygenation represent something real and do not, for instance, occur because of changes in cell density during the deoxygenation process. (It might have been the case that the N_2 gas used for deoxygenation caused evaporation and concentration of the sample.)

Noted in Table II is an increase in charge upon deoxygenation, evident in both the fresh and day-old RBCs. This is reasonable, as deoxyhemoglobin is known to have a higher affinity for protons than oxyhemoglobin, protons and oxygen molecules being antagonists that compete for the same binding sites (23). Since η is the same for both oxy and deoxy fresh RBCs, only the change in G_{ek} has an effect on $S'(Q)$, as illustrated in Fig. 9.

Fresh oxy and deoxy RBCs both show a value of $\eta \approx 0.223$ which is the same as that obtained for Hb in RBCs under "normal" salt conditions. As the cells age, η decreases for the oxy cells (see the day-old cells). Upon

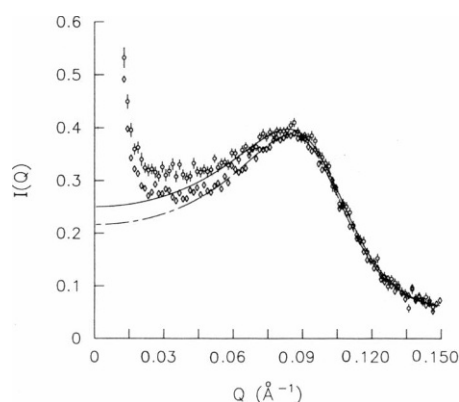


FIGURE 8 Changes in Hb cross-section noted when RBCs are deoxygenated. The lines represent the calculated Hb cross-section based on the parameters of best fit for $Q \geq 0.06 \text{ Å}^{-1}$. The background value for the deoxy cells has been normalized to that of the oxy cells. (----) Fresh oxy RBCs; (- - -) fresh deoxy RBCs. Error bars for deoxy data are similar to those shown for oxy data.

TABLE II
OXY AND DEOXY RED BLOOD CELLS
15% D_2O BUFFER pH 7.4

	η	Gek	Z	Amp	Bck
Fresh oxy cells	0.223	0.6	10	1.30	0.060(f)
Fresh deoxy cells	0.222	1.1	13	1.22	0.069(f)
Day-old oxy cells	0.215	0.4	8	1.30	0.028(f)
Day-old deoxy cells	0.222	0.7	11	1.25	0.036(f)
Reoxygenated oxy cells	0.207	0.1	4	1.33	0.030(f)
Reoxygenated deoxy cells	0.204	0.1	4	1.32	0.036(f)

R fixed at 28 Å , A_k fixed at 7.2. (f) denotes a "fixed" quantity for that particular fit. The "fixed" values were obtained from preliminary fits, in which Bck was allowed to vary. Fixing the values in later fits facilitated computation, and had no effect on the values obtained for the other parameters. The statistical errors associated with the fitting procedure are as follows: $\eta(\pm 0.002)$; Amp(± 0.01); Gek(± 0.1); Z(± 1).

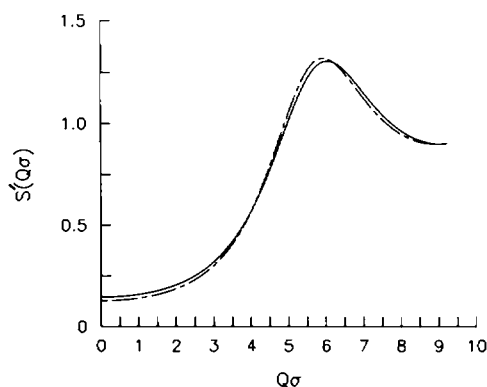


FIGURE 9 Calculated $S'(Q\sigma)$ for Hb in oxy and deoxy cells based on the parameters of best fit for $Q \geq 0.06 \text{ \AA}^{-1}$. (---) Fresh oxy RBCs; (—) fresh deoxy RBCs.

reoxygenation, η decreases again, for both samples. These changes may reflect variations in 2,3-diphosphoglycerate (DPG) levels within the cells as they age. From the SANS data alone, it is not possible to tell whether the average cell volume is increasing, or whether the degree of Hb association has changed. In any event, the volume changes would be much less than the rather large changes that seemingly would have to be invoked to explain results of recent microscope laser light scattering studies of the effects of oxygenation on the apparent diffusion of Hb in normal RBCs (8). The interpretation of the single-cell light scattering data is complicated by the possibility that a large amount of the discerned scattering may arise from the cell membranes (24, 25).

A small decrease in scattering amplitude was observed in the deoxy RBC samples (see Table II). This may be due to settling of the cells in the cuvettes. Unlike the samples for which the ionic strength of the solution was varied, no attempt was made to keep the number of cells per unit volume constant for both samples. If settling did occur, the only effect it would have on the data would be to lower the overall intensity of the scattering curve. While it is desirable to obtain the highest intensity possible, a lower number of cells per unit volume will not affect the interactions occurring between Hb molecules within each cell. On the other hand, the decrease in the average value of the background as the cells aged is significant and probably arises from H-D exchange between protein and solvent. Exchangeable hydrogen atoms in the molecules that are accessible will exchange with deuterium in the solvent. Since the solvent already consists of 85% H_2O , this additional hydrogen does not greatly affect the scattering of the buffer. Thus, when buffer scattering is subtracted from the total scattering, essentially the only remaining background is from hydrogen still within the cells. After H-D exchange, this amount is greatly reduced and, hence, a lower background value is obtained. This value should not change once exchange is complete, even after both samples are reoxygenated, in accordance with the data shown in

Table II. The small variation in the Bck values between oxy and deoxy cells may be due to slight differences in the dimensions of the cuvettes in which the samples were contained.

FURTHER REMARKS

A procedure for separately distinguishing between the scattering from core Hb and membrane has been described. When conditions are appropriate, the same methodology can be used to study other types of biological vesicles. The match point for the plasma membranes of other biological vesicles and cells will be similar to that for erythrocytes, and the experimental conditions that have been determined in the present study probably can be used as a first approximation.

If, however, the significant membrane and protein portions of the scattering curve overlap (e.g., when large protein particles or aggregates are present), the situation can be more complicated. In this instance it might be necessary to perform a contrast variation series on a preparation of membrane fragments in order to determine solvent conditions for the membrane match point. All subsequent measurements should be taken under those conditions but, since a true "match point" for the membranes does not exist, it still may be difficult to resolve the protein scattering. If, even at the membrane "match point," the protein scattering is not very much stronger than the membrane scattering, it may be necessary to devise a procedure for normalizing the scattering from a suspension of membranes to that from a suspension of intact vesicles. The two scattering profiles then could be compared, differentially, to determine whether or not the scattering cross-section contains a contribution from the protein.

The MSA fitting procedure has limitations that should be considered when analyzing the results of the fits. Because data were obtained in 15% D_2O in order to minimize membrane scattering, some precision in the protein data was sacrificed since the intensity of the protein scattering also is fairly low under those conditions. Certain parameters are sensitive to the range of Q values over which the fit is made: In particular, the fitted value of G_{ek} depends on the choice of the minimum Q value. On the other hand, R is not sensitive to changes in $I_p(Q)$ at smaller values of Q .

The fitted value of R thus is not useful for detecting aggregation. However, the apparent volume fraction, η , is extremely sensitive to changes in location and shape of the peak of the intensity curve, and therefore is a good measure of association between particles. That G_{ek} depends on the Q range over which data are fit implies that the exact values of the Hb electrostatic charge cannot be determined by this method (see Table II). However, the qualitative change in charge, noted when the cells are deoxygenated, is unaffected by varying the minimum value of Q . In most of the fits made for the Hb within the cell cores, A_k was the

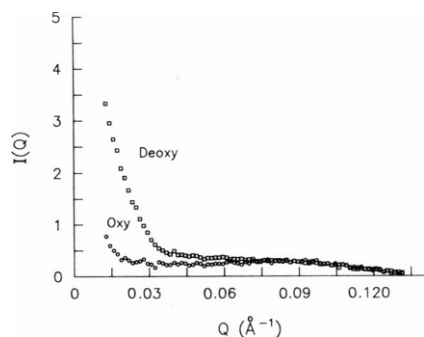


FIGURE 10 Scattering from sickle Hb RBCs in 10% D₂O, illustrating the detection of polymer formation when the cells are deoxygenated.

only known parameter, having been calculated to be that of the surrounding solution. Although R and B_{ck} could sometimes be fixed in later fits, five parameters initially were unknown. The ability to independently calculate an additional parameter would be helpful.

No attempt has been made in these studies to fractionate the RBC samples, although it is well known that the Hb concentration in the cells can vary quite significantly. Any serious study of RBC physiology should utilize more refined techniques of sample preparations. Here, however, we principally wanted to emphasize a methodology that can be used to study protein interactions within the interior of a variety of intact biological vesicles. An additional example, namely, sickle RBCs, is illustrated in Fig. 10. The data indicate a significant change in $I(Q)$ resulting from deoxygenation of the cells. The scattering at small values of Q represents the formation of long, fibrous sickle Hb polymers, while the peak near $Q = 0.09 \text{ \AA}^{-1}$ represents Hb monomers not involved in polymer formation. Note that the peak in the deoxy spectrum, appearing at low Q , is much broader than the membrane peak seen in Fig. 4 *a* for normal RBCs suspended in 10% D₂O.

Secretory vesicles and other biological organelles also are amenable to study by similar SANS techniques, although a lower ratio of core protein to membrane scattering may be a complicating factor. Improvements in instrumentation, namely, the implementation of cold neutron sources with high fluxes of long wavelength neutrons, should facilitate studies of the membranous structures of such particles.

This work is from a dissertation submitted to the Graduate School, University of Maryland, by Susan Krueger in partial fulfillment of the requirements for the Ph.D. degree in Physics.

Received for publication 31 March 1987 and in final form 28 September 1987.

REFERENCES

1. Nossal, R., C. J. Glinka, and S.-H. Chen. 1986. SANS studies of concentrated protein solutions. I. Bovine serum albumin. *Biopolymers*. 25:1157-1175.
2. Pardon, J. F., J. F. Worcester, J. C. Wooley, K. Tatchell, K. E. van Holde, and B. B. Richards. 1975. Low-angle neutron scattering from chromatin subunit particles. *Nucleic Acids Res.* 2:2163-2176.
3. Koch, M. H. J., and H. B. Stuhmann. 1979. Neutron-scattering studies of ribosomes. *Methods Enzymol.* 59:670-706.
4. Hayter, J. B., and J. Penfold. 1981. An analytic structure factor for macroion solutions. *Mol. Phys.* 42:109-118.
5. Hansen, J.-P., and J. B. Hayter. 1982. A rescaled MSA structure factor for dilute charged colloidal dispersions. *Mol. Phys.* 46:651-656.
6. Bendedouch, D., and S.-H. Chen. 1983. Structure and interparticle interactions of bovine serum albumin in solution studied by small-angle neutron scattering. *J. Phys. Chem.* 87:1473-1477.
7. Nishio, I., J. Peetermans, and T. Tanaka. 1985. Microscope laser light scattering spectroscopy of single biological cells. *Cell Biophys.* 7:91-105.
8. Peetermans, J., I. Nishio, S. Ohnishi, and T. Tanaka. 1986. Light-scattering study of depolymerization kinetics of sickle hemoglobin polymers inside single erythrocytes. *Proc. Natl. Acad. Sci. USA.* 83:352-356.
9. Glasoe, P. K., and F. A. Long. 1960. Use of glass electrodes to measure acidities in deuterium oxide. *J. Phys. Chem.* 64:188-190.
10. Dodge, J. T., C. Mitchell, and D. J. Hanahan. 1963. The preparation and chemical characteristics of hemoglobin-free ghosts of human erythrocytes. *Arch. Biochem. Biophys.* 101:119-130.
11. Glinka, C. J. 1982. AIP Conference Proceedings No. 89 (Neutron Scattering-1981). 395-397.
12. Glinka, C. J., and N. F. Berk. 1983. Position-Sensitive Detection of Thermal Neutrons. P. Convert and J. B. Forsyth, editors. Academic Press, Inc., New York. 141-148.
13. Chen, S.-H., and D. Bendedouch. 1986. Structure and interactions of proteins in solutions studied by small angle neutron scattering. *Methods Enzymol.* 130:79-116.
14. Egelstaff, P. A. 1967. An Introduction to the Liquid State. Academic Press, Inc., New York.
15. Waisman, E., and J. L. Lebowitz. 1972. Mean spherical model integral equation for charged hard spheres. I. Method of solution. *J. Chem. Phys.* 56:3086-3093.
16. Lin, T. L., and S.-H. Chen. 1985. FORTRAN Package 1,2,3. (Available from the authors on request.)
17. Krueger, S., and R. Nossal. 1986. MSA Fitting Program. (Available from the authors on request.)
18. Porod, G. 1982. General theory. Small Angle X-ray Scattering. O. Glatter and O. Kratky, editors. Academic Press, Inc., New York. 18-50.
19. Schelten, J., P. Schlecht, W. Schmatz, and A. Mayer. 1972. Neutron small angle scattering of hemoglobin. *J. Biol. Chem.* 247:5436-5441.
20. Hayter, J. B., and J. Penfold. 1981. Self-consistent structural and dynamic study of concentrated micelle solutions. *J. Chem. Soc. Faraday Trans. I.* 77:1851-1863.
21. Oosawa, F. 1971. Polyelectrolytes. Marcel Dekker Inc., New York.
22. Wu, C.-F., and S.-H. Chen. 1987. SANS studies of concentrated protein solutions: determination of the charge, hydration, and H/D exchange in cytochrome C. *J. Chem. Phys.* 87:6199-6205.
23. Dickerson, R. E., and I. Geis. 1983. Hemoglobin: Structure Function, Evolution and Pathology. Benjamin/Cummings Publishing Co., Menlo Park, California.
24. Tishler, R. B., and F. D. Carlson. 1987. Quasi-elastic light scattering studies of membrane motion in single red blood cells. *Biophys. J.* 51:993-997.
25. Tishler, R. B. 1987. Membrane associated and age related changes in human red blood cell membranes measured by quasi-elastic light scattering. *Biophys. J.* 51:515a. (Abstr.)